Supporting Information for

ORIGINAL ARTICLE

Intravenous route to choroidal neovascularization by macrophage-disguised nanocarriers for mTOR modulation

Weiyi Xia[a,†], Chao Li[b,†], Qinjun Chen[b], Jiancheng Huang[a], Zhenhao Zhao[b], Peixin Liu[b], Kai Xu[a], Lei Li[a], Fangyuan Hu[a], Shujie Zhang[a], Tao Sun[b], Chen Jiang[b,*], Chen Zhao[a,*]

[a]*Department of Ophthalmology and Vision Science, Eye & ENT Hospital, Shanghai Medical School, Fudan University, Shanghai 200031, China*

[b]*Key Laboratory of Smart Drug Delivery, Ministry of Education, Department of Pharmaceutics, School of Pharmacy, Fudan University, Shanghai 201203, China*

Received 17 August 2021; received in revised form 20 September 2021; accepted 15 October 2021

[*]Corresponding authors. Tel./fax: +86 21 51980079 (Chen Jiang); +86 21 64377134 (Chen Zhao).

E-mail addresses: jiangchen@shmu.edu.cn (Chen Jiang), dr_zhaochen@163.com (Chen Zhao).

[†] These authors made equal contributions to this work.

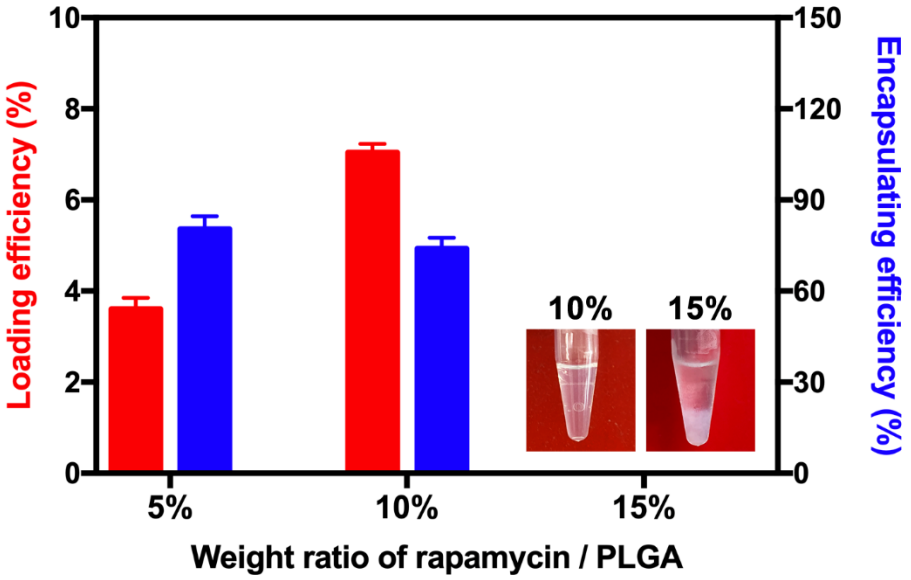

Figure S1 Optimization of drug loading in RaNP. The drug loading efficiency (LE) and the encapsulation efficiency (EE) of RaNP when different w/w of rapamycin (5%, 10%, and 15%) was added (n=3).

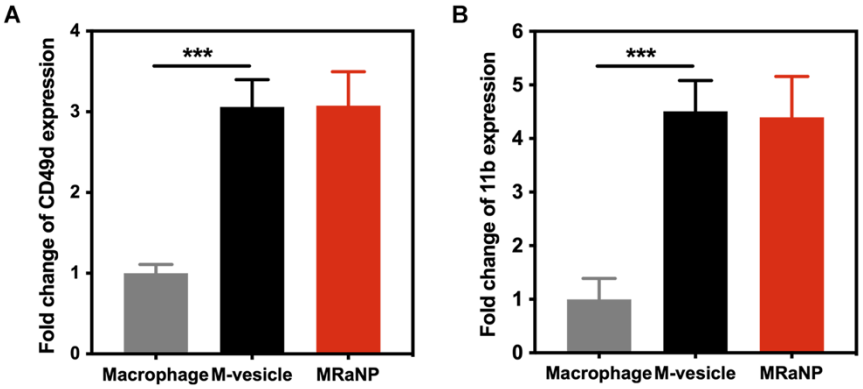

Figure S2 Semi-quantitation analysis of results in Figure 2I (***P<0.001).

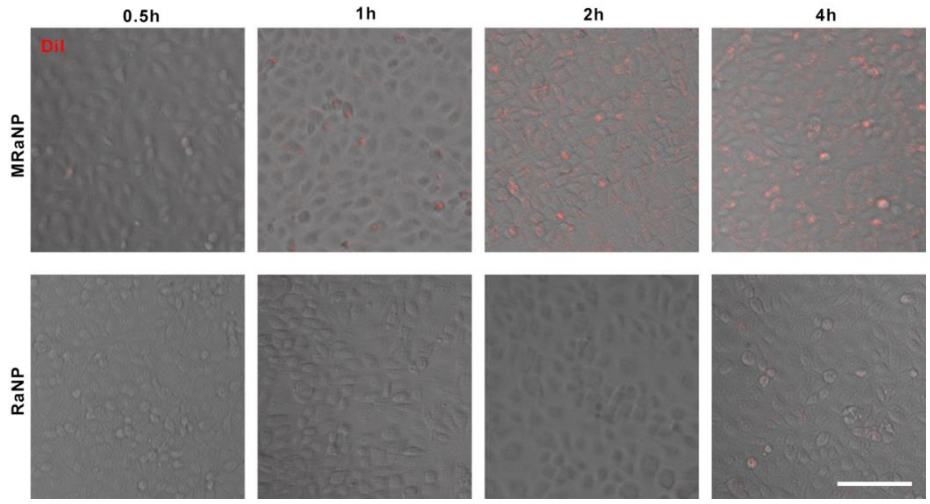

Figure S3 *In vitro* cellular uptake by endothelial cells. Representative fluorescence images of cellular uptake of DiI-labeled nanoparticles (red) by HUVECs at different time points. Scale bar=100 μm.

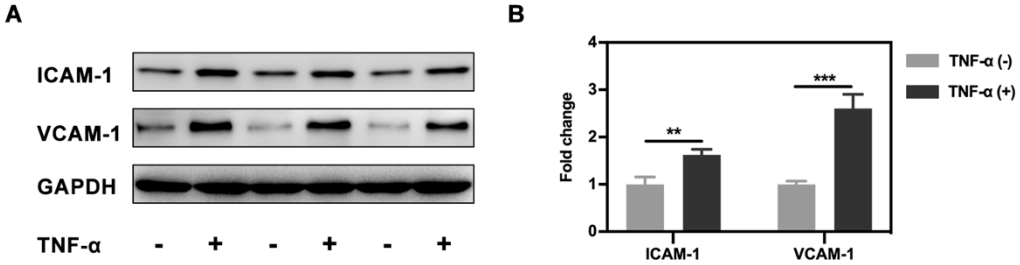

Figure S4 Expression of adhesion molecules *in vitro*. WB analysis (A) and semi-quantitation analysis (B) of ICAM-1 and VCAM-1 expression in HUVECs with or without TNF-*α* treatment (n=3, ***P*<0.01 and ****P*<0.001).

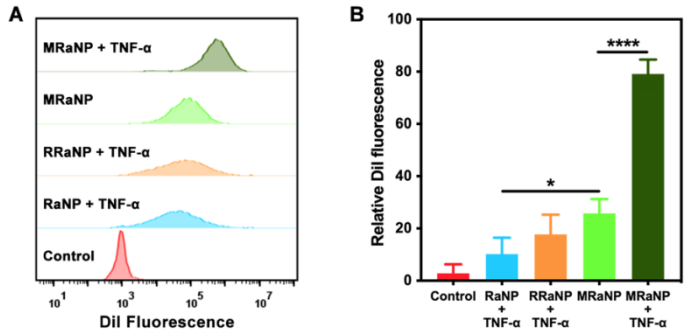

Figure S5 *In vitro* uptake of MRaNPs by HUVECs under inflammatory condition. Flow cytometry results (A) and quantitation analysis (B) of different formulations internalized by HUVECs in response to TNF-*α* stimulus (n=3, **P*<0.05 and *****P*<0.0001).

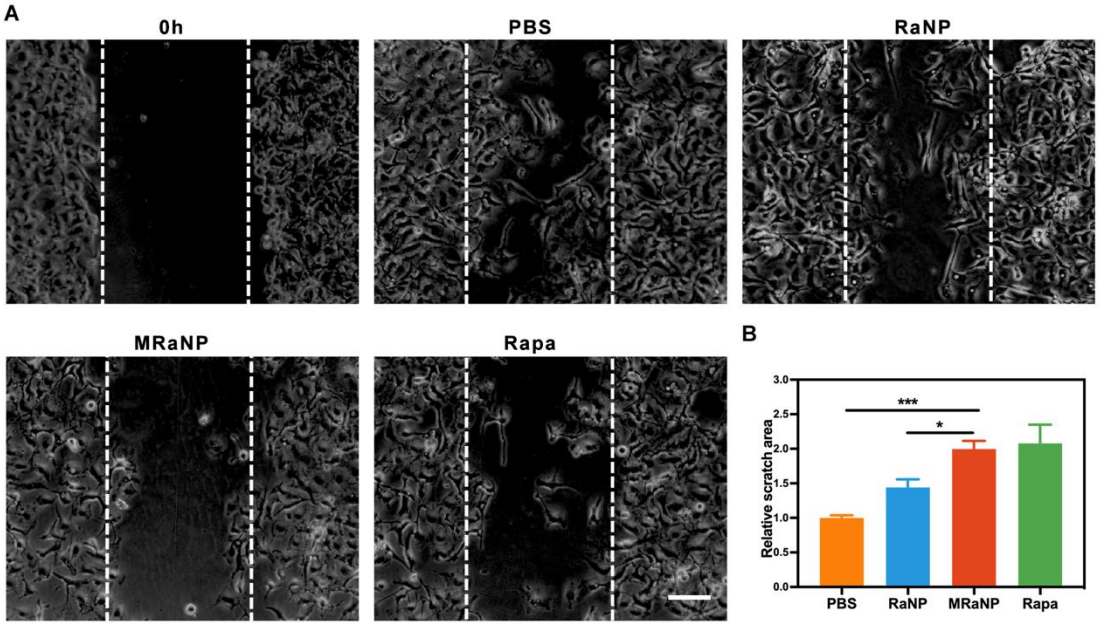

Figure S6 Scratch wound migration assay. (A) Representative images of effects on endothelial cell migration by MRaNPs. Scale bar=100 μm. (B) Quantitation analysis determined by relative scratch area (n=3, **P*<0.05 and ****P*<0.001).

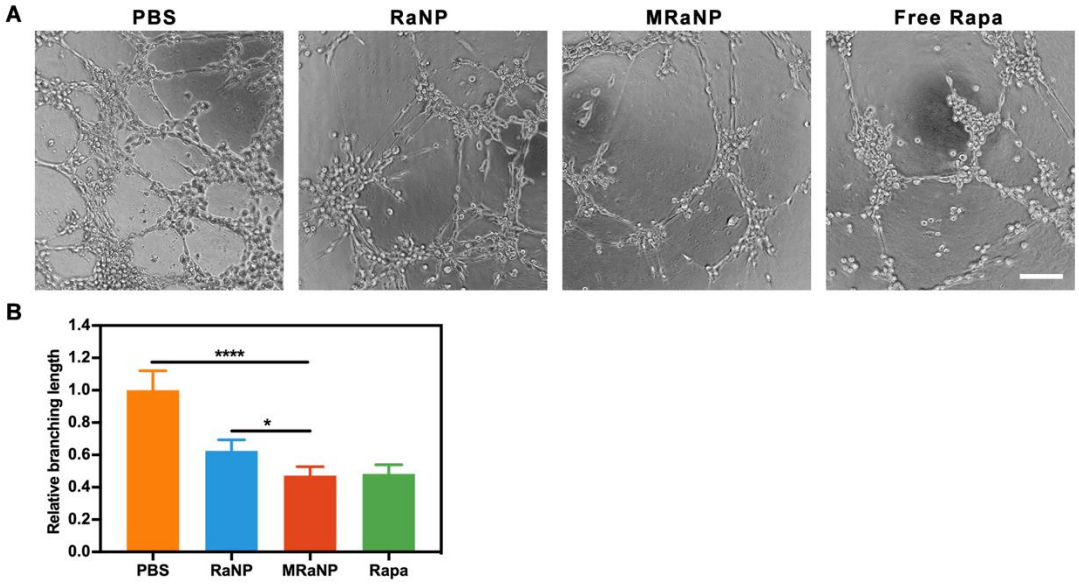

Figure S7 Tube formation assay. (A) Representative images of effects on endothelial cell tube formation by MRaNPs. Scale bar=100 μm. (B) Quantitation analysis determined by relative branching length (n=3, **P*<0.05 and *****P*<0.0001).

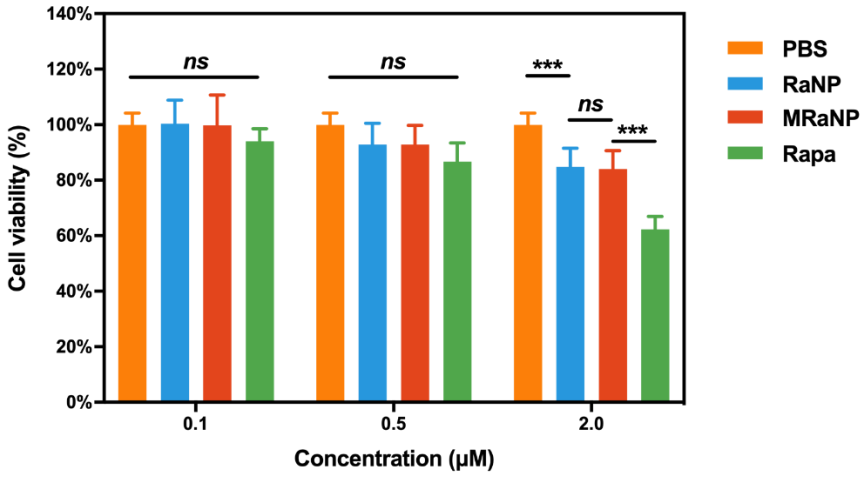

Figure S8 *In vitro* investigation on biocompatibility of MRaNPs by 24 h. Cell viability of ARPE-19 cells measured by CCK-8 assay kit (n=5, ***P<0.001. *ns*, not significant).

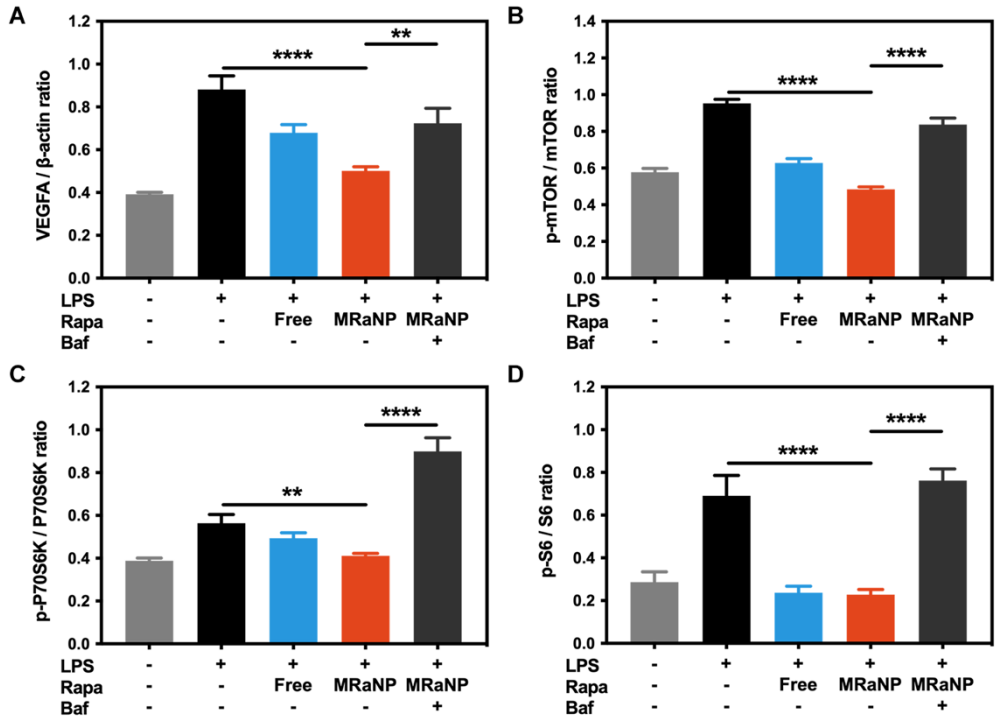

Figure S9 Semi-quantitation analysis of results in Figure 4B. (**P<0.01, ***P<0.001 and ****P<0.0001).

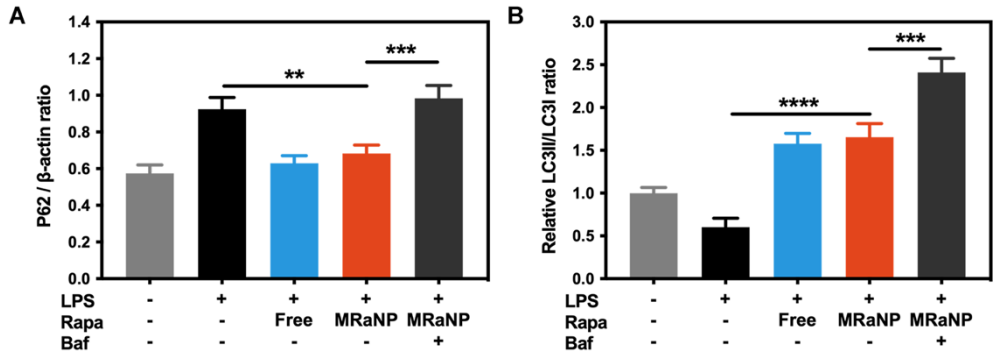

Figure S10 Semi-quantitation analysis of results in Figure 4G. (***P*<0.01 and *****P*<0.0001).

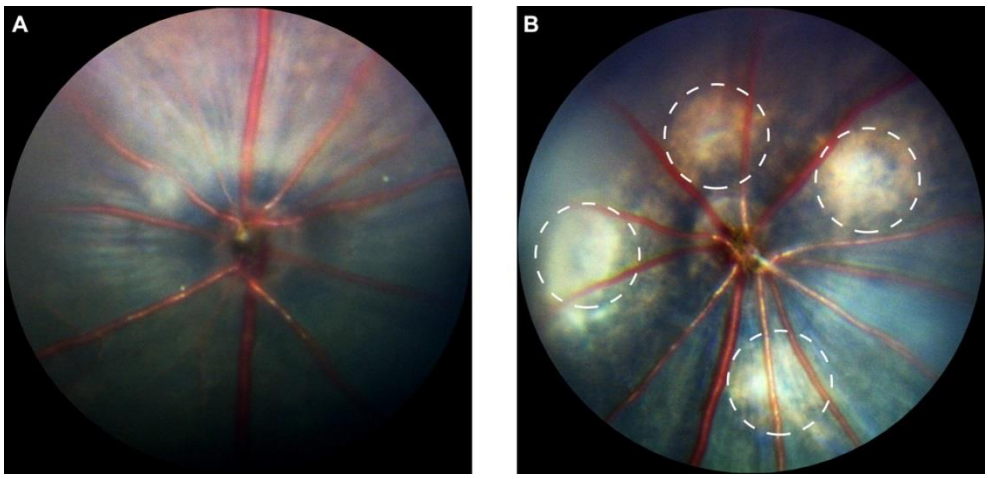

Figure S11 Representative fundus photographs of normal and LCNV mice. (A) Representative image of normal fundus. (B) Representative image of LCNV fundus with 4 laser burns shown as bright white spots. Dashed lines delineate the lesion.

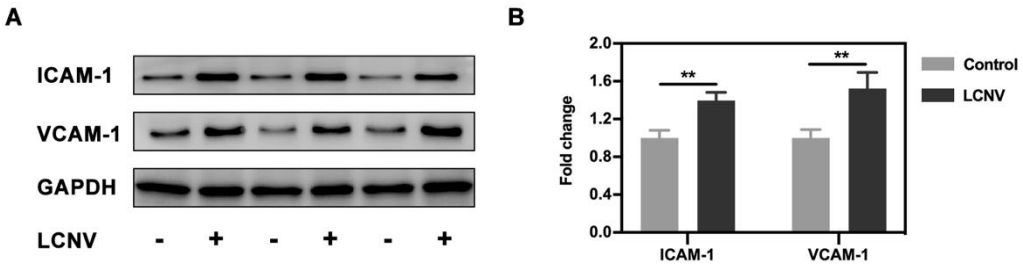

Figure S12 Expression of adhesion molecules *in vivo*. WB analysis (A) and semi-quantitation analysis (B) of ICAM-1 and VCAM-1 expression in the RCCs from mouse with or without laser treatment (n=3, ***P*<0.01).

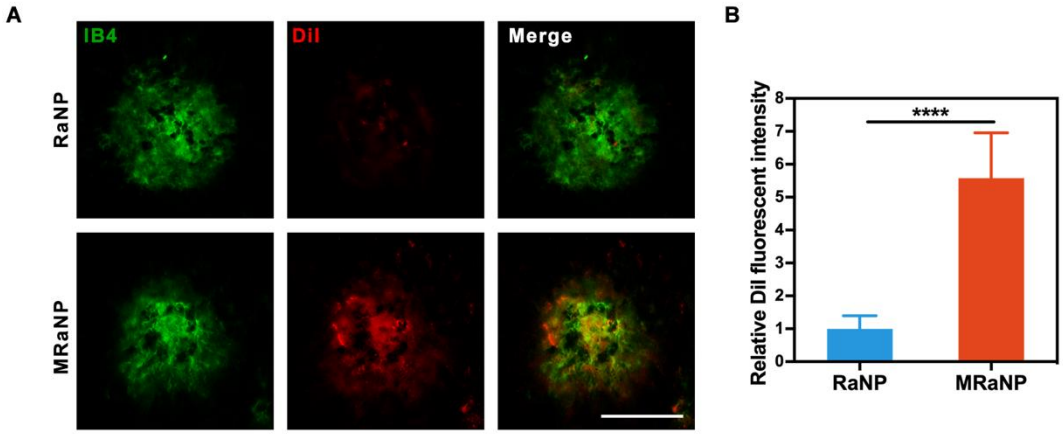

Figure S13 *In vivo* CNV-targeting ability of MRaNPS by flat-mounted RCCs. (A) Representative fluorescence images showing DiI-labeled nanoparticles (red) in CNV areas stained by IB4 (green). Scale bar=100 μm. (B) Quantitation analysis of DiI fluorescence intensity (n=5, ****P<0.0001).

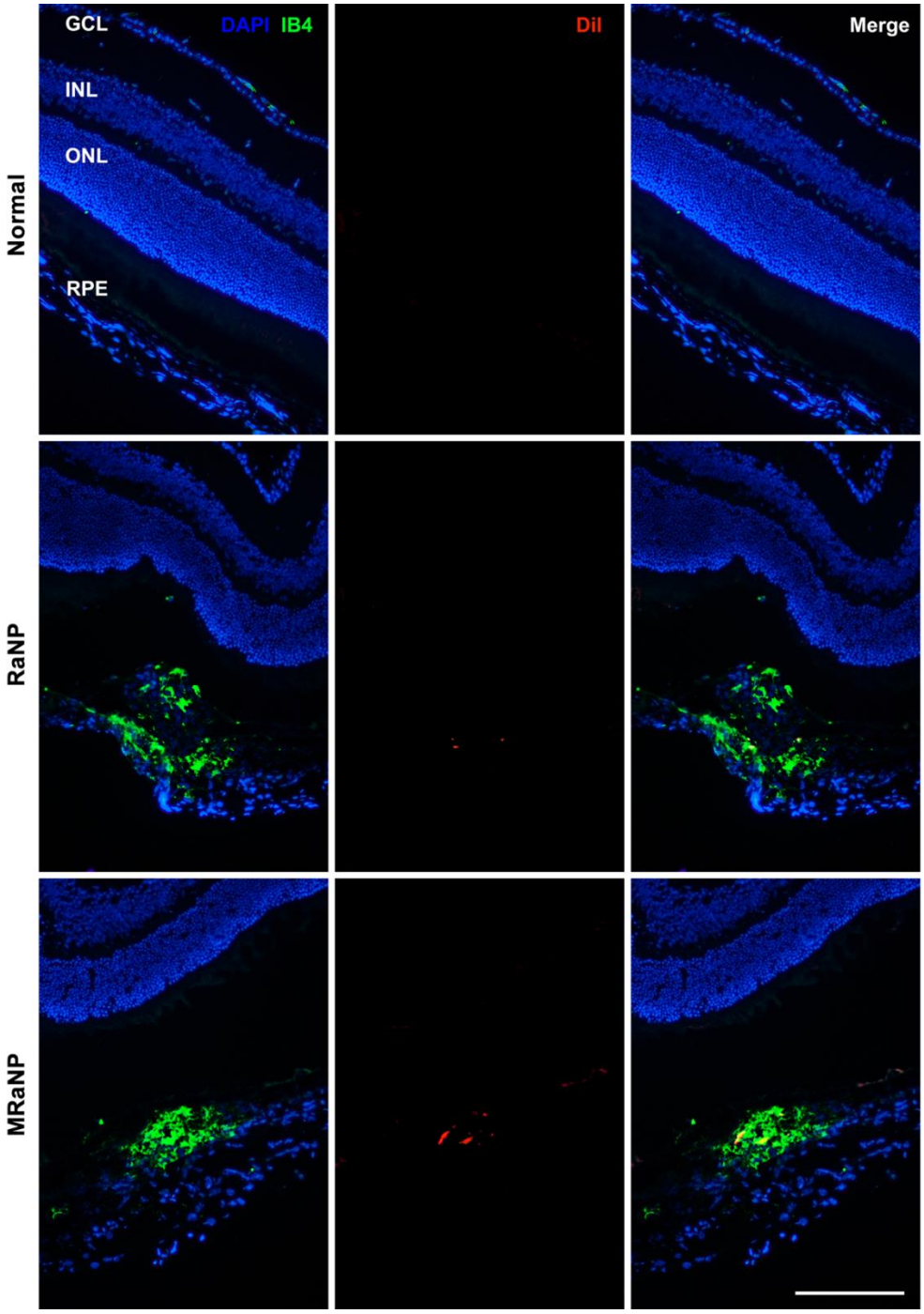

Figure S14 *In vivo* CNV-targeting ability of MRaNPs by transverse retina sections. Representative fluorescence images showing DiI-labeled nanoparticles (red) in CNV areas stained by IB4 (green). ONL, outer nuclear layer; INL, inner nuclear layer; GCL, ganglion cells layer. Scale bar=50 μm.

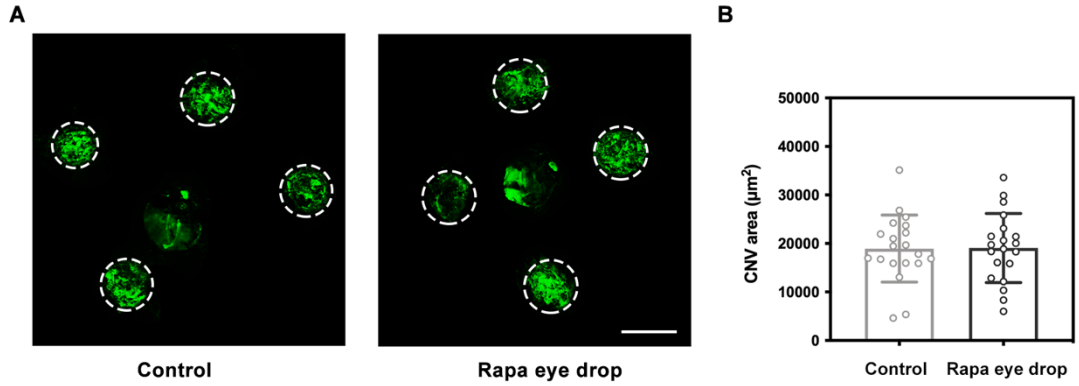

Figure S15 Therapeutic efficacy of topical administration of Rapa in the LCNV mouse model. (A) Representative fluorescence images of in CNV areas stained by IB4 (green) with or without Rapa eye drop treatment. Dashed lines delineate the lesion. Scale bar=100 μm. (B) Quantitation analysis of CNV areas (20 laser points each group, no statistical significance).

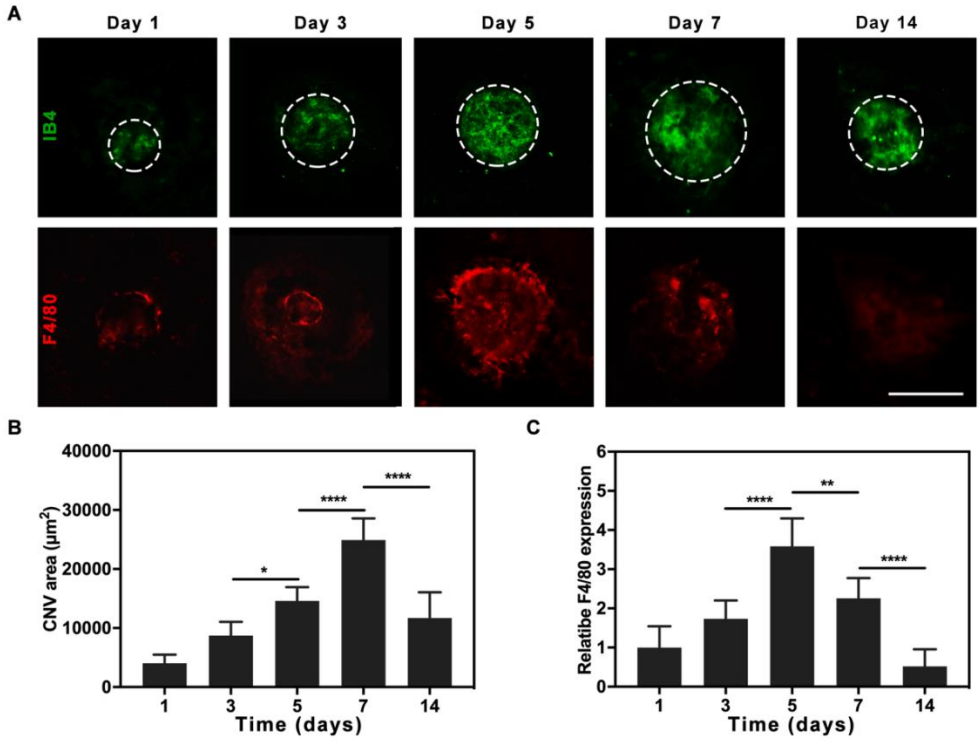

Figure S16 Natural time-course of CNV formation and macrophage infiltration in LCNV mice. (A) Representative fluorescence images of immunostaining of F4/80 (red, macrophage marker) in CNV areas stained by IB4 (green) at different time points after laser treatment. Dashed lines delineate the lesion. Scale bar=100 μm. (B and C) Quantitation of CNV areas and F4/80 fluorescence intensity at different time points (n=5, **P*<0.05, ***P*<0.01, ****P*<0.001 and *****P*<0.0001).

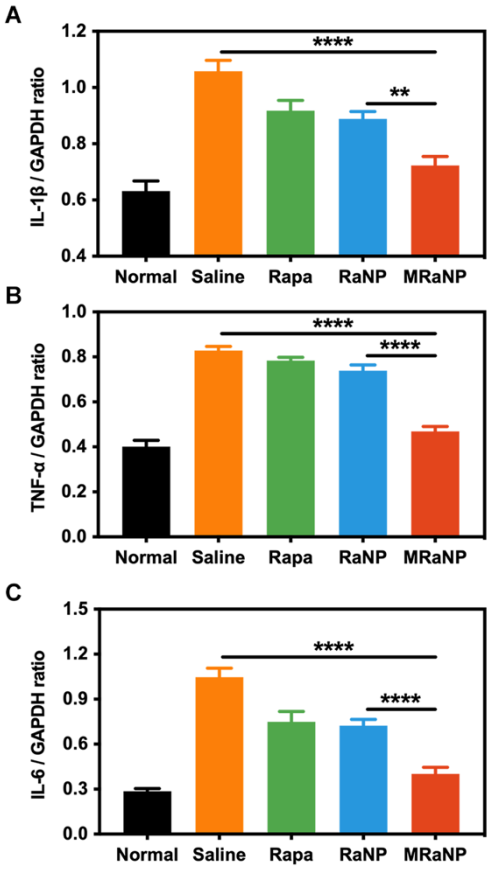

Figure S17 Semi-quantitation analysis of results in Figure 5E (***P*<0.01 and *****P*<0.0001).

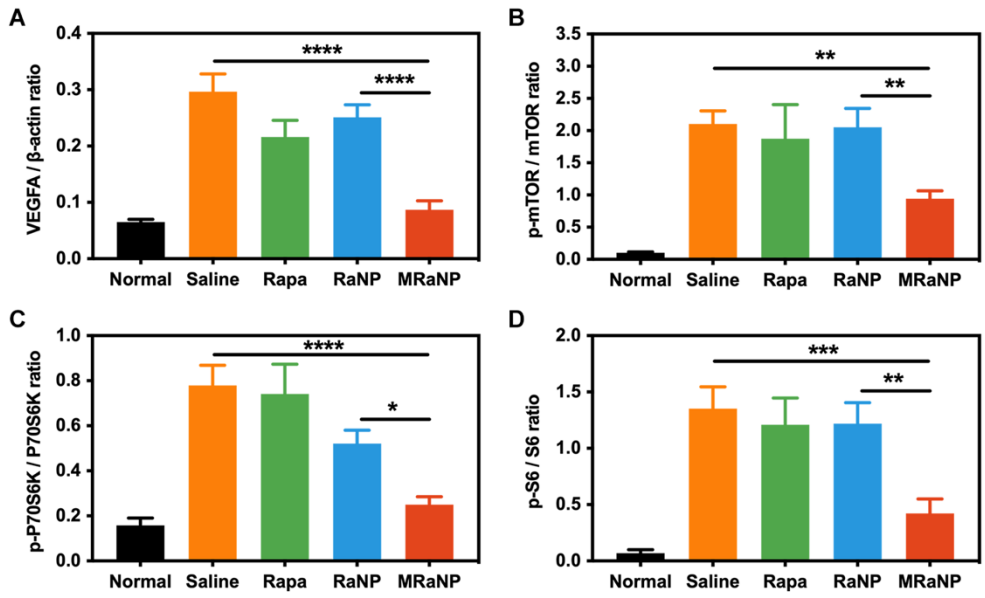

Figure S18 Semi-quantitation analysis of results in Figure 6A (**P*<0.05, ***P*<0.01, ****P*<0.001 and *****P*<0.0001).

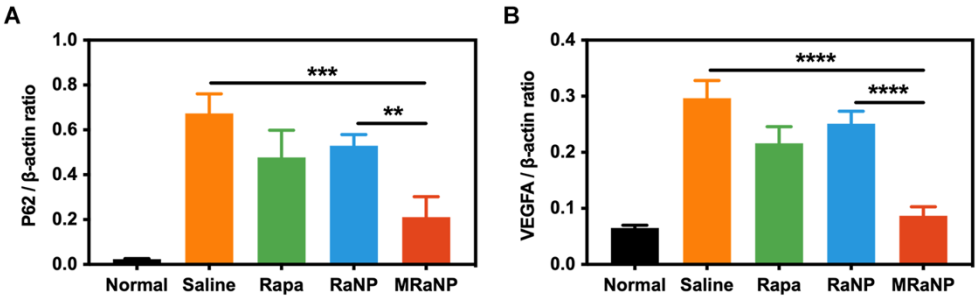

Figure S19 Semi-quantitation analysis of results in Figure 6D (***P*<0.01, ****P*<0.001 and *****P*<0.0001).

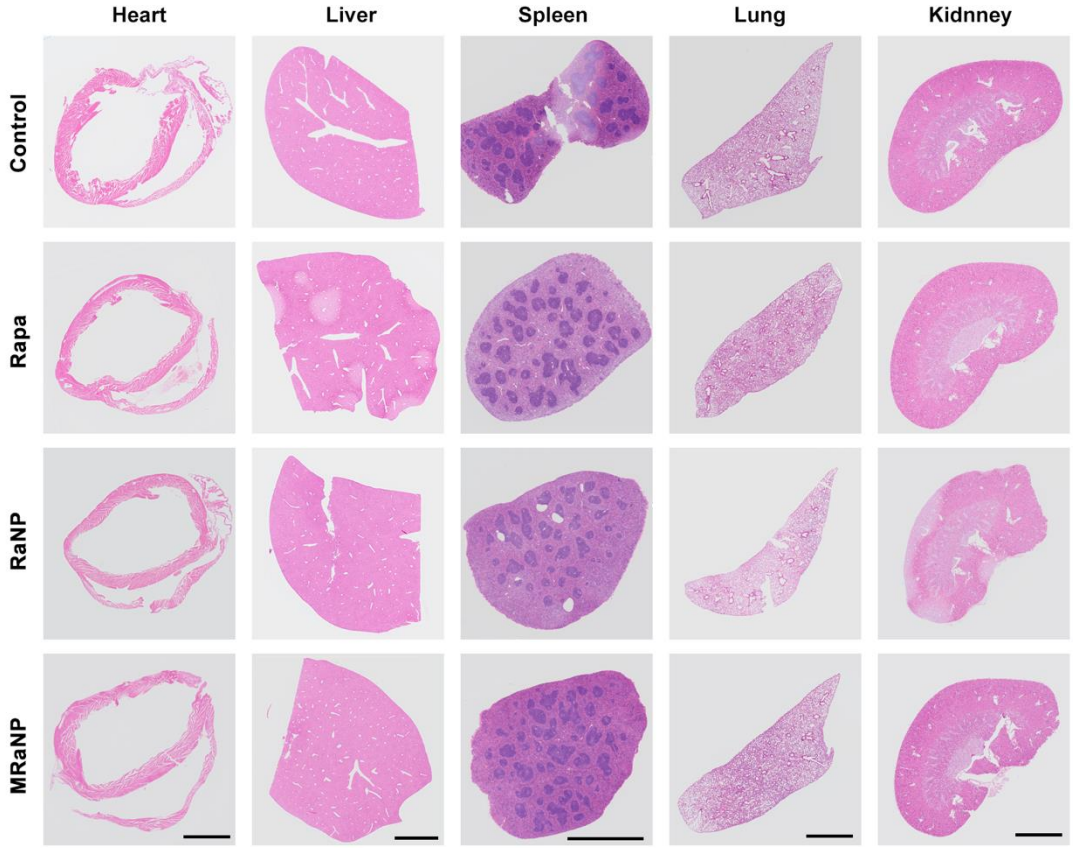

Figure S20 H&E staining of whole major organs after different treatment. Representative images of major organs by H&E staining indicated no tissue damage on Day 8. Scale bar=2 mm.

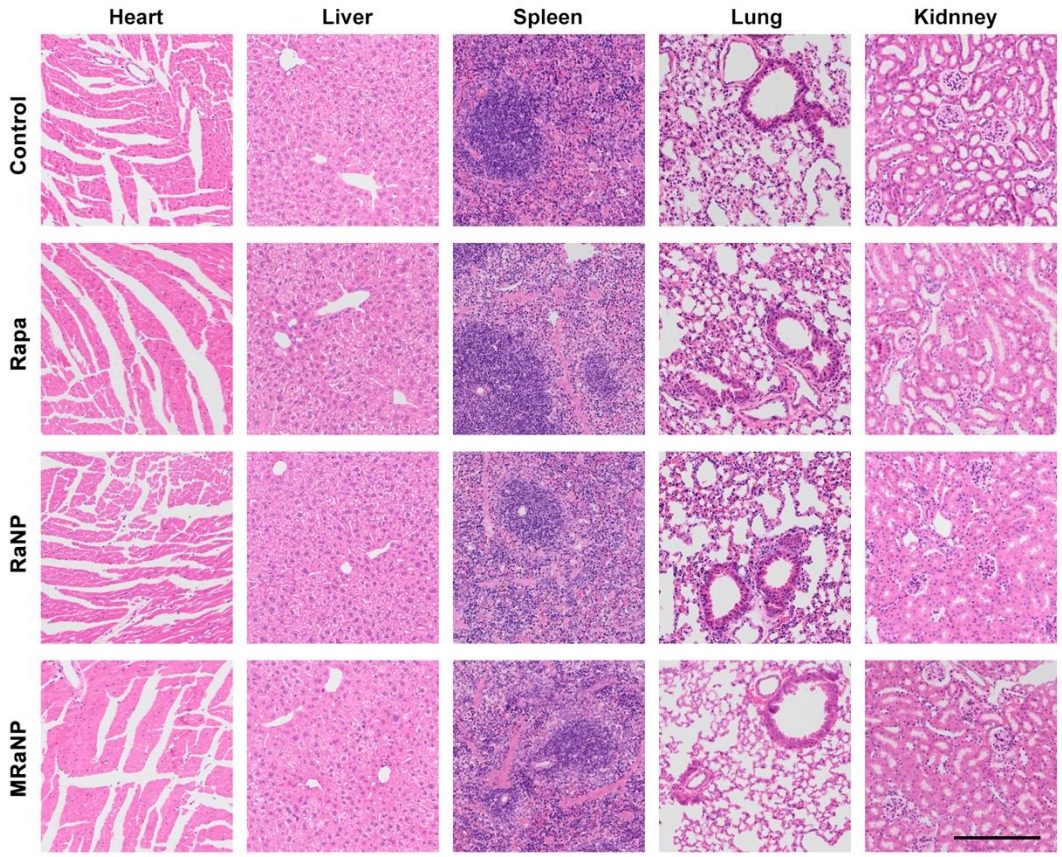

Figure S21 H&E staining of major organs after different treatment. Representative images of major organs by H&E staining indicated no tissue damage on Day 8. Scale bar=200 μm.